Title
Cation Exchange: A Versatile Tool for Nanomaterials Synthesis

Journal
The Journal of Physical Chemistry C, 117(39)

ISSN
1932-7447

Authors
Beberwyck, Brandon J.
Surendranath, Yogesh
Alivisatos, A. Paul

Publication Date
2013-10-03

THE JOURNAL OF PHYSICAL CHEMISTRY C

Feature Article

pubs.acs.org/JPCC

Cation Exchange: A Versatile Tool for Nanomaterials Synthesis

Brandon J. Beberwyck,[†,§] Yogesh Surendranath,[‡,∥] and A. Paul Alivisatos*[,†,‡,§]

[†]Department of Materials Science and Engineering and [‡]Department of Chemistry, University of California, Berkeley, California 94720, United States

[§]Materials Sciences Division, Lawrence Berkeley National Laboratory, Berkeley, California 94720, United States

[∥]Miller Institute for Basic Research in Science, University of California, Berkeley, California 94720, United States

ABSTRACT: The development of nanomaterials for next generation photonic, optoelectronic, and catalytic applications requires a robust synthetic toolkit for systematically tuning composition, phase, and morphology at nanometer length scales. While de novo synthetic methods for preparing nanomaterials from molecular precursors have advanced considerably in recent years, postsynthetic modifications of these preformed nanostructures have enabled the stepwise construction of complex nanomaterials. Among these post-synthetic transformations, cation exchange reactions, in which the cations ligated within a nanocrystal host lattice are substituted with those in solution, have emerged as particularly powerful tools for fine-grained control over nanocrystal composition and phase. In this feature article, we review the fundamental thermodynamic and kinetic basis for cation exchange reactions in colloidal semiconductor nanocrystals and highlight its synthetic versatility for accessing nanomaterials intractable by direct synthetic methods from molecular precursors. Unlike analogous ion substitution reactions in extended solids, cation exchange reactions at the nanoscale benefit from rapid reaction rates and facile modulation of reaction thermodynamics via selective ion coordination in solution. The preservation of the morphology of the initial nanocrystal template upon exchange, coupled with stoichiometric control over the extent of reaction, enables the formation of nanocrystals with compositions, morphologies, and crystal phases that are not readily accessible by conventional synthetic methods.

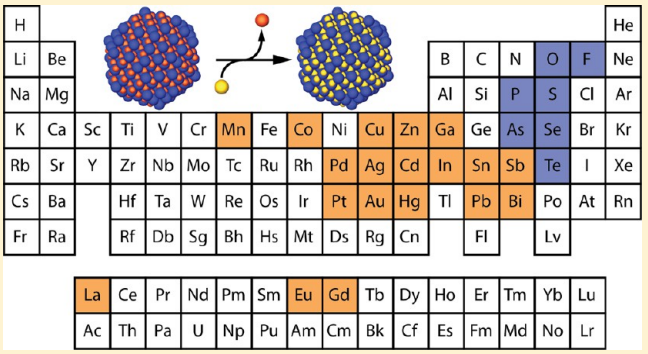

INTRODUCTION

The physical and chemical properties of periodic extended solids change drastically as the crystallite size is reduced to nanometer dimensions.[1] A quantitative understanding of these fundamental scaling laws has emerged as a direct result of synthetic advances that permit the preparation of monodisperse crystallites of diverse nanoscale size and shape. The direct synthesis of nanocrystal colloids is most practically achieved using a hot-injection protocol, in which molecular precursors are rapidly decomposed at elevated temperatures to produce a burst of nanocrystal nucleation followed by uniform steady-state growth.[2,3] Hot-injection synthetic methods have proven particularly powerful for accessing monodisperse II−VI and IV−VI compound semiconductor nanocrystals. Indeed, a wide array of morphological diversity can be achieved among the II−VI class of nanocrystals and has enabled their widespread utilization in optoelectronic,[4] photocatalytic,[5] and bioimaging[6] applications.

Direct nanocrystal synthesis methods require a careful tuning of nucleation, growth, and surface ligation kinetics at temperatures sufficient to crystallize phase-pure extended solids.[2,3] All of these kinetic processes remain poorly understood, and as a consequence, there remain no *general* design principles for the de novo synthesis of a nanocrystal of arbitrary composition, phase, morphology, or surface structure. However, synthetic protocols have been extensively refined for several classes of compound semiconductor nanocrystals which may serve as general anion host lattices for the preparation of compositionally diverse, morphologically well-defined nanomaterials provided that postsynthetic methods for cation substitution can be broadly applied. Recent developments suggest that a postsynthetic cation exchange strategy might prove particularly versatile for the synthesis of large classes of binary nanocrystalline phases that would otherwise be inaccessible by application of direct hot-injection synthetic methods.[7] In this article, we highlight the thermodynamic and mechanistic basis for cation exchange reactions at the nanoscale and use this as a backdrop to illustrate selected applications of cation exchange for the preparation of nanocrystals that are challenging to access by direct synthesis from molecular precursors. For a broader view of cation exchange in nanostructures including applications beyond synthesis, we direct the readers to a recent tutorial review.[8]

Received: June 17, 2013
Revised: August 23, 2013
Published: September 3, 2013

   dx.doi.org/10.1021/jp405989z | *J. Phys. Chem. C* 2013, 117, 19759−19770

FUNDAMENTALS OF CATION EXCHANGE AT THE NANOSCALE

Ion exchange, the substitution of ions in an extended solid with those in solution, is an age-old strategy for modifying the composition and properties of crystalline materials. Ion substitution reactions are responsible for various re-equilibration processes in rocks[9] and displacement reactions in metal oxides[10] and, of more technological relevance, serve as a simple processing technique for thin-film semiconductors.[11] In particular, cation exchange of thin-film semiconductors has been utilized to form a broad range of structures including optical waveguides, heterojunctions for optoelectronic devices, and alloys for infrared photodetectors.[11]

In recent years, cation exchange reactions have been increasingly applied as a synthetic tool for accessing novel nanomaterials. For both nanocrystalline colloids and bulk extended solids, a typical cation exchange procedure is extremely simple. For example, exposing nanocrystal colloids of CdSe to a methanolic solution of Ag^+ ions leads to rapid formation of Ag_2Se colloids with liberation of Cd^{2+} from the reactant host lattice (Figure 1).[7] Microscopically, each individual cation substitution reaction can be viewed as the extended solid analogue of transmetalation reactions commonly observed for molecular coordination compounds.[12] In addition to their simplicity, nanoscale cation exchange reactions typically exhibit excellent morphology retention, rapid reaction rates, and tunable thermodynamics making them a particularly attractive synthetic tool. While complementary anion exchange reactions have also been demonstrated,[13−15] the larger size and lower diffusivity of lattice anions lead to sluggish reaction kinetics and poor morphology retention, often giving rise to hollow nanostructures.[16]

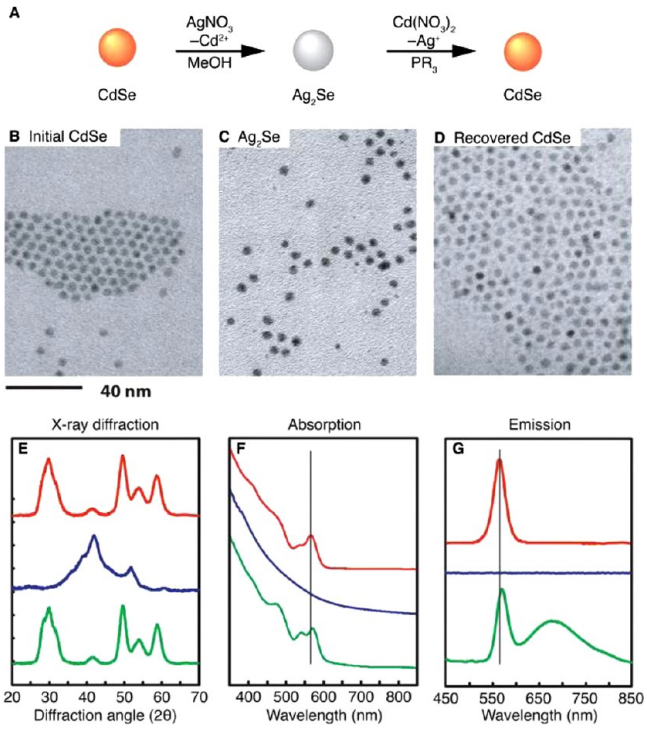

Figure 1. (A) Reaction scheme for the conversion of CdSe to Ag_2Se and Ag_2Se to CdSe. Exposure of CdSe to a methanolic solution of Ag^+ leads to the rapid formation of Ag_2Se. Ag_2Se is exchanged back to CdSe by exposure of the Ag_2Se nanocrystals to excess Cd^{2+} in the presence of a trialkyl phosphine. TEM images of (B) as-synthesized CdSe nanocrystals, (C) Ag_2Se nanocrystals synthesized via cation exchange, and (D) CdSe nanocrystals recovered from the reverse cation exchange reaction. XRD patterns (E), absorption spectra (F), and emission spectra (G) of initial CdSe (red), Ag_2Se (blue), and recovered CdSe (green) nanocrystals, respectively. Adapted with permission from ref 7, copyright 2005 AAAS.

While a cation exchange reaction is remarkably simple to execute, the outcome of the reaction and the structure of the product obtained are dictated by subtle thermodynamic and kinetic factors. First among these are the relative thermodynamic stabilities of the reactant and product phases. Second are the relative thermodynamics of cation solvation and/or specific ligation in the liquid phase. While these two parameters, cation solvation and phase stability, can predict, to a first approximation, the thermodynamic feasibility of an overall ion exchange reaction, they provide little insight into the reaction pathway or the structure of the product. Since ion exchange reactions must proceed through partially substituted alloy intermediates, the thermodynamics of the *interphase* between reactant and product phases, referred to as the exchange reaction zone, dictates the structure and morphology of the product crystallite. While these principles apply to solid-state ion exchange reactions broadly, regardless of crystallite size, we will use contemporary examples of ion exchange reactions at the nanoscale to illustrate the importance of bulk, solution, and interfacial thermodynamics in dictating the reaction outcome.

Kinetic factors are also key in determining the feasibility of an ion exchange reaction. In this respect, the kinetics of ion exchange at the nanoscale differ substantially from those observed for bulk extended solids because limits on long-range solid-state ion diffusion are significantly relaxed by the large surface-to-volume ratios of nanoscale crystallites. Indeed, solid-state diffusion limitations in bulk crystallites often necessitate the application of high temperatures and pressures to achieve rapid product formation.[11] As an example, Ag^+, which possesses a relatively high ion diffusivity,[17] sluggishly converts a thin film (500 nm) of CdSe to Ag_2Se, requiring several hours at 80 °C,[18] whereas the similar reaction in CdSe nanocrystals (see above) proceeds to completion in ≪1 s at room temperature.[7] In the subsequent section, we will highlight recent mechanistic studies of ion exchange kinetics at the nanoscale to illustrate the mechanistic consequences of relaxing limitations on solid-state ion diffusion.

THERMODYNAMICS OF CATION EXCHANGE

The synthetic feasibility of a cation exchange reaction is determined by its net thermodynamic driving force and intervening activation barriers.[19] For cation exchange to become a general synthetic tool, a quantitative understanding of the thermodynamics of the exchange process is desired to permit the rational design of future exchange reactions. Consider, for example, an arbitrary ion exchange reaction between two metal sulfides

$$AS + B^{2+} \leftrightarrows BS + A^{2+} \quad (1)$$

where A and B represent divalent metal ions. This overall exchange reaction can be divided into two hypothetical electrochemical half reactions

$$AS \leftrightarrows A^{2+} + 2e^- + S^0 \quad (2)$$

dx.doi.org/10.1021/jp405989z | J. Phys. Chem. C 2013, 117, 19759−19770

Table 1. Calculated Aqueous Reaction Free Energies Per Sulfur Equivalent, $\Delta G^0_{reaction}$ (kJ mol^{-1}), for the Cation Exchange of Reactant (Abscissa) To Product (Ordinate) Metal Sulfides

Product \ Reactant	PdS	HgS	Ag_2S	Cu_2S	SnS	PbS	CdS	ZnS	NiS
PdS	0	−33.8	−55.5	−63.5	−169.0	−176.8	−182.1	−198.7	−214.6
HgS		0	−21.7	−29.7	−135.2	−143.0	−148.3	−165.0	−180.8
Ag_2S			0	−8.0	−113.5	−121.3	−126.6	−143.2	−159.1
Cu_2S				0	−105.5	−113.3	−118.6	−135.2	−151.1
SnS					0	−7.8	−13.1	−29.8	−45.6
PbS						0	−5.3	−21.9	−37.8
CdS							0	−16.6	−32.5
ZnS								0	−15.9
NiS									0

$$B^{2+} + 2e^- + S^0 \leftrightarrows BS \quad (3)$$

each of which may be further decomposed into the corresponding standard free energy of formation (ΔG^0_f) of each phase and the standard reduction potential (E^0) of the metal ion in question

$$AS \rightleftarrows A^0 + S^0 \quad -(\Delta G^0_f)_{AS} \quad (4)$$

$$A_0 \rightleftarrows A^{2+} + 2e^- \quad -(E^0)_{A^{2+}} \quad (5)$$

$$B^0 + S^0 \rightleftarrows BS \quad (\Delta G^0_f)_{BS} \quad (6)$$

$$B^{2+} + 2e^- \rightleftarrows B_0 \quad (E^0)_{B^{2+}} \quad (7)$$

Thus, for this example, the overall aqueous driving force for ion exchange (eq 1) is given by

$$\Delta G_{reaction} = (\Delta G^0_f)_{BS} - (\Delta G^0_f)_{AS} - 2F[(E^0)_{B^{2+}} - (E^0)_{A^{2+}}] \quad (8)$$

where F is Faraday's constant. Since tabulated formation energies[20] are available for a number of binary chalcogenides, oxides, and pnictides and aqueous redox potentials[21] are known for virtually every metal ion in the periodic table, the aqueous thermodynamics of any given ion exchange reaction can be readily calculated.[22] We wish to stress that this strategy provides a convenient method for calculating ion exchange thermodynamics but does not imply anything about the mechanistic pathway by which ion exchange proceeds. Using this simple methodology, aqueous driving forces are presented in Table 1 for a select number of metal sulfide phases.

The foregoing discussion highlights the two key determinants of ion exchange thermodynamics: the difference in formation energies of the reactant and product phases and the difference in redox potentials of the exchanging ions. For simplicity, the above calculation and the values in Table 1 take into account only the bulk lattice formation energies for each phase and aqueous redox potentials for the attendant metal ions. In practice, the thermodynamic driving force for an ion exchange may significantly differ from these estimates for the following two principle reasons.

First, nanostructuring is expected to significantly depress the formation energies of each phase. Formation energies for the product and reactant colloid may be highly dependent on crystallite size and shape, and significant thermodynamic contributions to phase stability may arise from ligands bound to the surface of the nanocrystal. If these energy contributions scale unevenly between the reactant and product phase, the actual thermodynamics of an exchange reaction may deviate significantly for the values calculated in Table 1. These effects are expected to be particularly pronounced for very small crystallites (<2 nm), in which a majority of the metal ions reside on the surface.

Second, the ligating environment in solution is expected to significantly alter the reduction potential of each metal ion.[23] While readily accessible aqueous redox potentials provide a starting point for estimating ion exchange free energies, these potentials are known to vary significantly, depending on the

dx.doi.org/10.1021/jp405989z | J. Phys. Chem. C 2013, 117, 19759−19770

solvating/ligating environment of the solution in which the exchange occurs. As a consequence, the thermodynamic preference for a given ion exchange can be easily reversed (Figure 1) if the ions discharged from the reactant lattice can be *preferentially* ligated in solution. A ligand's propensity for selective ion binding can be qualitatively understood in the context of Pearson's hard soft acid base (HSAB) theory, which classifies Lewis acids and bases by varying degrees of hardness, η, based on their polarizability.[24] Hardness serves as a qualitative predictor of selective ion binding because like interactions, hard−hard and soft−soft, are favored relative to opposing, soft−hard, interactions. This principle has been exploited to drive the replacement of soft Ag^+ (η = 6.96 eV) and Cu^+ (η = 6.28 eV) ions in chalcogenide host lattices with harder metal ions including Cd^{2+} (η = 10.29 eV),[7] Zn^{2+} (η = 10.88 eV),[25,26] and Pb^{2+} (η = 8.46 eV)[27] via preferential ligation to soft tertiary phosphines ($\eta \sim 6$ eV). This strategy has, thereby, enabled both reversible and sequential exchanges.

While a quantitative assessment of nanostructuring and specific ligation effects awaits detailed thermochemical studies of nanoscale cation exchange reactions, the above crude calculations can provide a starting point for designing ion exchange synthetic protocols that take advantage of intrinsic thermodynamics or preferential ion ligation.

MECHANISTIC INSIGHTS INTO NANOSCALE CATION EXCHANGE

While thermodynamic considerations can serve to guide the development of new cation exchange syntheses, many of these reactions proceed under nonequilibrium conditions, necessitating a careful consideration of the mechanistic pathways by which they proceed. While a detailed microkinetic description of solid-state cation exchange remains elusive, qualitative mechanistic pathways have been proposed for these reactions in minerals[9] and thin-film semiconductors.[11] For ion exchanges in semiconductor thin films, which are most analogous to the corresponding reactions in colloidal nanocrystals, appreciable rates of heterogeneous ion substitution at crystallite surfaces and rapid solid-state diffusion of the exchanging cation are required. Experimental results indicate that the rate of diffusion within each crystallite is typically much slower than the rate of substitution at the crystallite surface. Thus, the composition at the surface of the substrate remains in quasi-equilibrium and is dictated by the solution composition and temperature, independent of the time duration of the reaction. The disparity between the surface and bulk composition during a cation exchange establishes a chemical potential gradient within the film, providing a driving force for directional diffusion of the replacing ion in the parent lattice. Reaction progress is then kinetically limited by the rate of solid-state diffusion. Indeed, the compositional profile of a thin film undergoing a cation exchange can be used to measure the self-diffusion coefficients of the constituent ions, finding good agreement with values determined by established radiotracer techniques.[11]

In both mineral replacement reactions and semiconductor thin-film ion exchange, the transport of ions to the boundary between reactant and product phases is believed to be the rate-limiting step.[9,11] The ion exchange reaction can then be viewed as the propagation of this phase boundary across the crystallite. In this fashion, ion exchange reactions can be described by analogy to the solid-state heterophase concept of a reaction zone.[28] The reaction zone, typically a several atomic layer thick region between two materials, represents a local variation in the chemical composition and charge distribution relative to either bulk phase.

The stability and propagation of the reaction zone have direct consequences for particle size-dependent morphology retention during a nanocrystal cation exchange.[7] For example, nanorod morphology retention is strongly dependent on the rod diameter for CdSe to Ag_2Se ion exchange reactions (Figure 2). Small diameter (~3.5 nm) CdSe nanorods transformed into

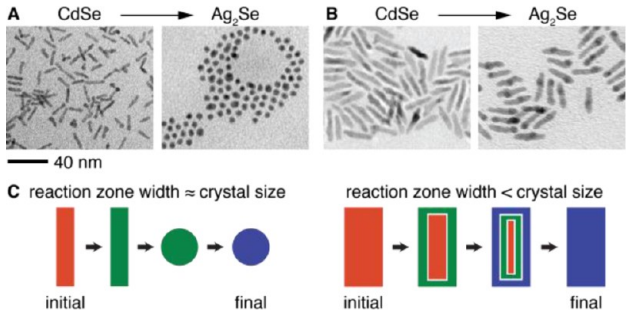

Figure 2. TEM images of CdSe nanorods and the product Ag_2Se nanocrystals for (A) small diameter nanorods in which the reaction zone is comparable to the crystallite dimensions and (B) large diameter nanorods in which the reaction zone is significantly smaller than the crystallite dimensions. (C) Schematic of size-dependent morphology changes during the CdSe to Ag_2Se exchange reaction. Orange and blue colors indicate the regions of initial reactant and final product phase, respectively. The green region indicates the reaction zone. Adapted with permission from ref 7, copyright 2005 AAAS.

spherical Ag_2Se nanocrystals upon Ag^+ exchange (Figure 2A), whereas larger diameter (~5 nm) CdSe nanorods maintained their morphology upon conversion to Ag_2Se (Figure 2B). These results can be rationalized if we invoke a reaction zone on the order of 3 nm in diameter. For thin nanorods, wherein the reaction zone dimensions are comparable to the particle diameter, the entire structure will reside in a nonequilibrium state during the exchange such that both cations and anions can rearrange to generate the thermodynamically preferred, spherical morphology (Figure 2C). However, if the size of the nanocrystal is significantly larger than the reaction zone, only a portion of the crystallite experiences significant structural distortions during the exchange, while the remainder of the lattice remains intact, templating retention of the nanorod morphology (Figure 2C). In this fashion, the anion sublattice is subject to minimal net reorganization over the course of the exchange if the crystal size is much larger than the dimensions of the reaction zone.

When nanoscale crystallites are large enough to preserve anionic framework stability, the crystal structure and nanoscale morphology remain robust, as demonstrated by performing forward and reverse exchanges between CdSe → Ag_2Se → CdSe.[7] As a result of quantum confinement, CdSe nanocrystals exhibit a characteristic excitonic absorption and narrow emission band that is highly sensitive to the size of the particle. Through sequential forward and reverse exchanges that serve to regenerate the starting phase, the absorption and emission maxima remain largely unchanged, indicating that the crystallite size and anion stoichiometry remain largely invariant during the cation exchange process (Figure 1E, F). The same phenomenon has been observed for exchanges conducted on nanoheterostructures, consisting of a CdSe sphere embedded in a CdS rod.[29] Ion substitution with Cu^+ was followed by

dx.doi.org/10.1021/jp405989z | J. Phys. Chem. C 2013, 117, 19759−19770

reintroduction of Cd^{2+} to regenerate the initial CdSe/CdS core−shell heterostructure. Through this series of ion exchange reactions, negligible shifts in the photoluminescence peak maxima were observed indicating preservation of the Se core sublattice within the S anion shell sublattice. Additionally, minimal structural and compositional changes were observed by scanning transmission electron microscopy high angle annular dark field (STEM-HAADF) imaging. These results establish that for sufficiently large crystallites cation exchange reactions can effectively preserve the size, position, and interfacial structure of one or more anion sublattices.

While cation exchanges can be executed for material systems with very high volume changes, in the extreme limit, crystallite size is a key determinant of morphology retention. This was directly investigated in the case of ion exchange from cadmium to platinum and palladium chalcogenides, CdE → Pt_xE_y, P_xdE_y (E = S, Se, Te).[19] For each chalcogenide, this exchange reaction is accompanied by a substantial contraction of the unit cell volume ($\Delta V/V \sim -30\%$). By comparison, the canonical CdSe → Ag_2Se exchange results in a <1% change in the unit cell volume ($\Delta V/V < 1\%$). The ability of the host lattice to accommodate large volume changes is highly dependent on crystallite size. Small spherical nanocrystals conserved their original morphology and transformed into a kinetically frozen metastable state until thermally annealed. However, the additional stress accumulated in larger spherical particles and anisotropic rod structures reached a critical point such that void formation or fragmentation occurred during the exchange to relieve stress due to the extreme lattice mismatch.

The above examples showcase the end point structures that result from cation exchange. On the pathways toward these products, the interfacial thermodynamics of the reaction front define the structures of alloy intermediates. By directly probing the alloy structures that result from partial ion substitution in a nanocrystal host, mechanistic insights into the site selectivity of initiation and propagation of the reaction front have been revealed.

Cation exchanges of CdS nanorods with fast diffusing monovalent ions (Cu^+, Ag^+) provide a clear example of the unique nature of the initiation and propagation of cation exchange reactions among nanocrystals.[30−32] As these reactions are highly exergonic at room temperature and exhibit facile kinetics,[33] the extent of reaction can be easily controlled by introducing substoichiometric amounts of the substituting ion. Since CdS is largely immiscible with Ag_2S and Cu_2S,[34,35] incomplete exchange of CdS with Cu^+ or Ag^+ will lead to phase-segregated CdS−Cu_2S and CdS−Ag_2S alloy structures. However, the heterostructures produced during incomplete exchange are remarkably different for copper vs silver (Figure 3A−D), highlighting the disparate interfacial formation energetics of the two systems. These differential energetics include contributions from the chemical formation energies at each heterophase junction and lattice strain contributions arising from epitaxial mismatch.

The chemical formation energy, reflecting the strength of the Cd−S−Ag bond, is negative for the Ag_2S−CdS interfaces.[31] Thus, for Ag^+ exchange of CdS nanorods, low Ag^+ concentration leads to the nonselective nucleation of Ag_2S islands embedded along the periphery of the CdS nanorod, showing no preference for nucleation at specific facets (Figure 3A). However, epitaxy of the orthorhombic Ag_2S and wurtzite CdS phases requires a 4% expansion of the Ag_2S lattice along the plane of the interface and a 15% contraction perpendicular

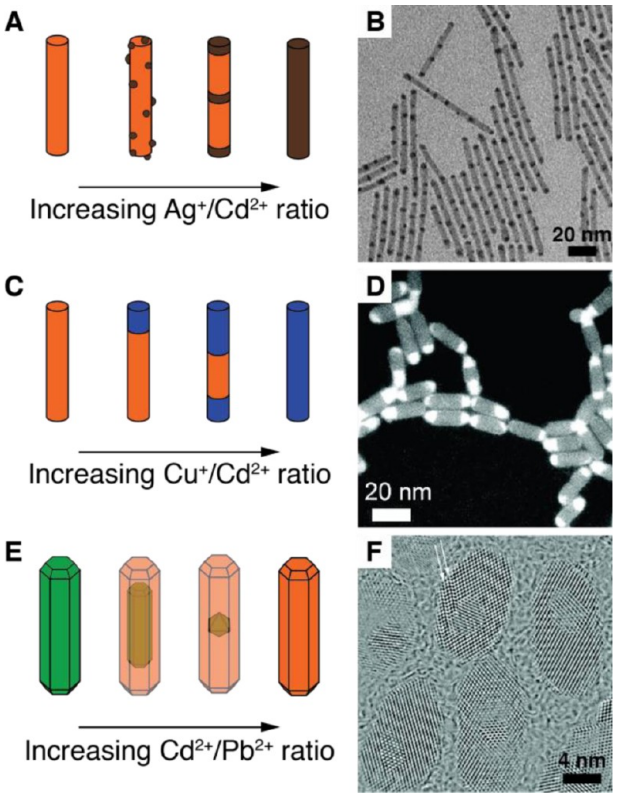

Figure 3. (A) Schematic of the progressive exchange of CdS nanorods with Ag^+. (B) TEM image of CdS−Ag_2S nanorods formed from partial Ag^+ exchange displaying superlattices. Adapted with permission from ref 30, copyright 2007 AAAS. (C) Schematic of the progressive exchange of CdS nanorods with increasing Cu^+ concentration. (D) Cu energy filtered TEM image of CdS−Cu_2S binary nanorods. The bright regions in the images correspond to Cu_2S, and the gray regions correspond to the CdS portions of the nanorods. Adapted with permission from ref 31, copyright 2009 American Chemical Society. (E) Schematic of the progressive exchange of PbSe nanorods with increasing Cd^{2+} concentration. (F) High-resolution TEM images of PbSe nanorods at the intermediate stage of Cd^{2+} exchange, displaying rock salt PbSe dots embedded in a zinc blende CdSe rod. Adapted with permission from ref 37, copyright 2012 American Chemical Society.

to it, adding an elastic strain energy contribution to the formation energy.[30,32] As the Ag^+ exchange progresses, these Ag_2S islands begin to grow, increasing the elastic strain in the Ag_2S segments. Eventually, the elastic strain results in a positive total interfacial formation energy of the Ag_2S−CdS segments, causing the larger Ag_2S islands to absorb the smaller ones by Ostwald ripening, facilitated by the high diffusivity of the Ag^+. Once the Ag_2S segments have spanned the diameter of the CdS rod, the Ag_2S−CdS regions spontaneously self-order due to the elastic repulsion between neighboring segments of Ag_2S arising from the lattice-mismatch-induced strain field (Figure 3B).[30−32] Upon addition of more Ag^+, the Ag_2S segments become larger until the entire CdS structure has been transformed into Ag_2S.

In contrast, positive chemical interface formation energies of Cu_2S−CdS and small elastic contributions from nearly identical sulfur sublattices lead to a strongly facet-dependent exchange of CdS nanorods with Cu^+ (Figure 3C, D).[31] Epitaxial chemical formation energy calculations show that Cu_2S attachment to the $(000\bar{1})$ facet of CdS, parallel to the rod cross-section, leads to the lowest-energy interface, whereas attachment to the

dx.doi.org/10.1021/jp405989z | J. Phys. Chem. C 2013, 117, 19759−19770

opposing (0001) facet entails a 2.5 times larger energy penalty. These unfavorable interface energies dictate that interfacial surface area is minimized and aligned perpendicular to the long axis of the CdS rod. In agreement, at low Cu^+ concentration, nucleation of Cu_2S appears at the $(000\bar{1})$ end facet of the CdS rod, forming a Cu_2S–CdS interface parallel to the rod cross-section. As the Cu^+ exchange progresses with the addition of Cu^+, this interface continues to propagate along the length of the rod while maintaining its orientation. At even higher Cu^+ concentration, the nucleation of Cu_2S on the opposite end of the rod ((0001) CdS) begins and progresses, though these two Cu_2S regions maintain high asymmetry, consistent with the difference in formation energies of these two interfaces (Figure 3D). These Cu_2S regions continue to propagate until they meet and the entire rod has been exchanged.

The propagation of the reaction front can also be observed in the isovalent exchange of PbE → CdE (E = S, Se, Te).[36] In contrast to Ag^+ and Cu^+ exchange reactions of CdE, this reaction exhibits a larger activation barrier, permitting facile control over the reaction progress by incrementally adjusting the reaction temperature. The partial conversion of PbSe → CdSe on faceted PbSe nanocrystals including cubes, stars, and rods displayed similar progression of exchange, implying that this conversion is not preferentially nucleated by selective adsorption of the Cd at specific facets.[37] However, similar to the Cu^+ exchange, the propagation of the Cd^{2+} exchange appears to be strongly facet dependent, proceeding in a strongly anisotropic ⟨111⟩ direction, leading to the formation of primarily {111} interfaces between the zinc blende CdSe and rock salt PbSe (Figure 3E,F).[37−39] As each {111} layer consists of only Cd, Pb, or Se, a sharp interface boundary between these immiscible phases may be achieved by propagation along the ⟨111⟩ direction. The highly anisotropic nature of this reaction leads to the formation of octahedral cores of PbSe within a CdSe rod when subject to partial ion exchange.

Relative to their bulk crystalline analogues, the reduced volume of nanoscale materials significantly relaxes the kinetic demands of solid-state diffusion. For example, using bulk diffusion coefficients,[17] Ag^+, Cu^+, and Au^+ ions can diffuse the entire length of a 5 nm diameter InAs crystal in less than a second at ambient temperature.[40,41] Thus, the diffusion-mediated propagation of the reaction zone may no longer be rate limiting for many nanoscale cation exchange reactions.[7] Indeed, time-resolved micro-X-ray absorption spectroscopy (XAS) and stopped flow absorption measurements of the topotaxial Ag^+ exchange of 3.5 nm CdSe nanocrystals indicate rapid conversion ($t_{1/2}$ < 100 ms), a strong dependence on the concentration of the coordinating ligand, and second-order kinetics consistent with a rate-limiting surface reaction step.[33] The short time scale and low activation energy (estimated to be 5 kcal mol^{-1}) emphasize the dramatically accelerated kinetics on the nanoscale. While a detailed mechanistic understanding of nanoscale cation exchange reactions awaits further study, the evidence accumulated thus far suggests that the reactions bear more kinetic resemblance to transmetalation reactions of molecular coordination complexes than bulk solid-state transformations. As anticipated, the kinetics of ion exchange transition from molecular-like to bulk-like behavior as the crystallite size increases. This transition has been observed for 30 nm diameter CdSe nanowires that exhibit solid-state diffusion-limited kinetics for Ag^+ substitution.[42]

The isovalent exchange of PbE → CdE (E = S, Se, Te)[36] appears to exhibit a significantly larger activation energy than the Ag^+ exchange. The reaction is self-limiting, forming a shell of the exchanged material, which serves to impede further ion substitution. The reaction rate appears to follow typical Arrhenius behavior for a temperature-dependent activation process. These strongly temperature-dependent kinetics, as well as the layer-by-layer nature of the exchange (see above), imply a vacancy-assisted diffusion mechanism.[37,38]

SYNTHETIC VERSATILITY OF CATION EXCHANGE

Recent advances in colloidal nanoparticle synthesis have provided access to a vast library of high-quality monodisperse semiconductor, metal, and metal oxide nanocrystals, with exquisite control of size and morphology.[3,43,44] By in large, these nanocrystals have been prepared by a hot-injection synthesis from molecular precursors, wherein delicate control over precursor decomposition kinetics, nanocrystal nucleation and growth rates, and surfactant binding energies is required to achieve size and shape control.[2,3] This is especially true for the synthesis of morphologically anisotropic nanoparticles which rely heavily on facet-selective surfactant binding[43,45] and precise control over crystallographic polymorphism.[44] No general rules exist for achieving this across broad classes of materials. Thus, despite the exquisite size and shape control accessible for certain materials systems via hot-injection methods, such as II–VI semiconductors, there remain large classes of nanomaterials for which morphology-controlled syntheses remain elusive.

Cation exchange is a powerful tool for circumventing many of these challenges because morphological well-defined nanocrystals, prepared by traditional hot-injection methods, can be used as anion templates for the preparation of compositionally diverse pure and alloy phases that would be inaccessible by direct methods. In this section, we review recent applications of cation exchange to synthesize covalent phases, metastable nanostructures, multicomponent alloys, and doped nanocrystals that are all inaccessible by direct synthetic methods. We conclude with examples in which cation exchange is combined in situ with hot-injection strategies to generate complex nanomaterials in a simple, one-pot procedure.

Synthesis of Covalent Nanocrystal Phases. Whereas numerous direct synthetic methods exist for accessing monodisperse II–VI semiconductor nanocrystals, hot-injection syntheses of III–V nanocrystals fail to generate nanoparticles with narrow size dispersity and high crystallinity. Unlike their II–VI analogues, III–V semiconductors exhibit highly covalent lattices, requiring relatively high temperatures to access crystalline materials. However, the molecular precursors available for the direct synthesis of III–V nanocrystals decompose rapidly at low temperature. Thus, it has proven difficult to balance high precursor reactivity with high crystallization temperatures to achieve sufficient temporal separation of nucleation and growth, a key requirement for the synthesis of monodisperse nanoparticles.[46] Indeed, mechanistic studies indicate rapid depletion of molecular precursors during III–V syntheses mandating that growth occurs via Ostwald ripening and gives rise to broad size distributions.[47]

Cation exchange methods have proven invaluable for overcoming this obstacle and have enabled the synthesis of monodisperse III–V nanocrystals including GaP and GaAs.[48] Utilizing monodisperse Cd_3As_2 and Cd_3P_2 nanocrystals as host anion lattices, III–V nanocrystals can be obtained by treatment with group 13 ions (In^{3+} or Ga^{3+}) at elevated temperature. The difference in lattice energy provides sufficient driving force for

dx.doi.org/10.1021/jp405989z | J. Phys. Chem. C 2013, 117, 19759−19770

the conversion of Cd_3E_2 → GaE, InE (E = P, As), while maintaining a narrow size distribution. This example illustrates the versatility of cation exchange for accessing monodisperse nanomaterials recalcitrant to traditional hot-injection methods.

Synthesis of Metastable Nanocrystals. The mild reaction conditions attendant to most cation exchange reactions enable the synthesis of nonequilibrium crystal morphologies inaccessible by direct hot-injection methods. As highlighted above, kinetically controlled morphologies including rods and tetrapods can be readily prepared among the cadmium chalcogenides and postsynthetically converted into silver or copper chalcogenides with excellent morphology retention by exposure to Ag^+- or Cu^+-containing solutions at room temperature.[7,31] Through preferential ligation of trialkyl phosphines to soft Ag^+ and Cu^+ ions, subsequent exchanges with Pb^{2+} or Zn^{2+} can be used to further extend these complex morphologies to the lead and zinc chalcogenides (Figure 4).[26,27] This cation exchange strategy, therefore, comprises a simple three-step synthetic route to anisotropic nanorod morphologies of isotropic crystal phases, such as rock salt PbS.[27]

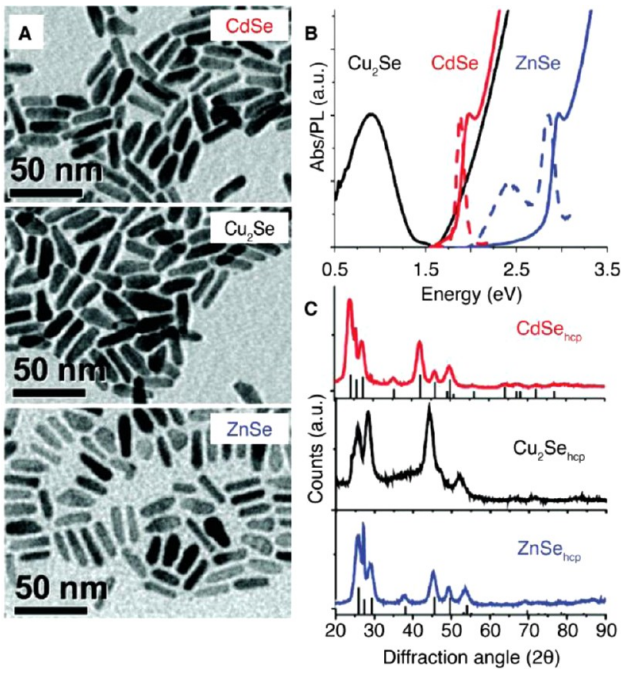

Figure 4. (A) TEM images of CdSe, Cu_2Se, and ZnSe nanorods and their corresponding (B) optical absorption/emission spectra and (C) XRD patterns. The morphology and crystal structure of the initial CdSe template is transferred to the Cu_2Se and ZnSe product nanocrystals. Adapted with permission from ref 26, copyright 2011 American Chemical Society.

Since cation exchange is a low-temperature, template-based synthetic method, it is well suited to the preparation of kinetically trapped, metastable crystal phases. The sequential exchange of CdSe → Cu_2Se → ZnSe nanocrystals transferred not only the size and shape of the parent nanocrystal but also the crystal structure (Figure 4).[26] Wurtzite CdSe was transformed to a metastable hexagonal close packed (HCP) phase of Cu_2Se by Cu^+ exchange, and subsequent exchange with Zn^{2+} yielded nanocrystals of ZnSe in the pure HCP phase. These examples illustrate that, in certain cases, the anion host lattice remains sufficiently rigid to template metastable product nanostructures with excellent crystallographic and morphological fidelity, independent of cation composition.

Synthesis of Alloy Nanocrystals. Exchange reactions in which only a fraction of the cations in the host lattice are replaced permit incremental compositional control and convenient access to both solid solutions and phase-segregated alloy nanocrystals. As II−VI compounds are known to form solid solutions with other group 12 ions,[11] partial exchange of II−VI nanocrystals with Cd^{2+}, Zn^{2+}, or Hg^{2+} can be used to form homogenously alloyed nanocrystals of constant morphology. This has enabled the investigation of the electronic structure of the nanocrystal as a function of composition at constant size. For instance, Hg^{2+} exchange of CdTe nanocrystals produces $Hg_xCd_{1-x}Te$ nanocrystals with incrementally tunable Hg content from 0 to 60% (x = 0−0.6).[49] The similar lattice parameters but distinct band gaps of CdTe and HgTe allow the absorption and fluorescence of the nanocrystals to be smoothly varied from the visible to near-infrared (NIR) by increasing the extent of Hg^{2+} substitution. Similarly, cation exchange induced alloying has been used to form ternary, $Cd_xZn_{1-x}Se$,[50] and quaternary, Cu−In−Zn--S,[51] chalcogenide nanocrystals.

Cation exchange methods are also well suited to the synthesis of phase-segregated alloy nanostructures, also known as nanoheterostructures.[52] A wide array of nanoheterostructures[53−57] have been synthesized by hot-injection methods, and these syntheses principally rely on seeded growth, in which a nanoparticle serves to induce the heterogeneous nucleation of the product phase, giving rise to a multicomponent product containing two or more phases in direct contact with each other.[52] Seeded growth protocols require exceptionally well-tuned precursor decomposition and growth kinetics to prevent parasitic homogeneous nucleation of the second phase and Ostwald ripening of the seed particles during the reaction.[36,52] Additionally, seeded growth protocol often requires registry between the lattices of the two materials to encourage efficient heterogeneous nucleation.[52]

Cation exchange provides an alternative approach for the formation of nanoheterostructures. At the most elementary level, complete cation exchange of a nanoparticle containing two anion sublattices can yield novel heterostructures difficult to access by direct synthetic methods. This has been demonstrated in the case of CdSe/CdS seeded rods, a unique class of heterostructures, in which the band alignment of the selenide and sulfide phases and the wavelength of emission can be tuned simply by changing the size of the CdSe seed.[56,57] Remarkably, treatment of CdSe/CdS heterostructures with Cu^+ generates Cu_2Se/Cu_2S heterostructures in which the anion sublattice has been largely undisturbed.[29,58] Subsequent treatment with Pb^{2+} or Zn^{2+} generates PbSe/PbS[29] and ZnSe/ZnS[58] seeded rods, respectively, providing opportunities for band engineering in the NIR and UV-blue region. Despite the low temperatures of these exchange reactions, the product nanoheterostructures are of high optical quality.[59]

Nanocrystals possessing a single anion host lattice can also serve as synthons for the preparation of nanoheterostructures via cation exchange. Provided that reactant and product phases are immiscible, partial cation exchange of a single-phase nanocrystal can generate a heterostructured product. This strategy affords significant advantages relative to traditional seeded growth methods because it obviates any complications that may arise from homogeneous nucleation of the product phase. As discussed above, the interfacial energetics of the two

dx.doi.org/10.1021/jp405989z | J. Phys. Chem. C 2013, 117, 19759−19770

coexisting phases dictate the propagation of the reaction zone, leading to various structural intermediates over the course of a cation exchange reaction. By choosing a starting nanocrystal of appropriate composition, morphology, and crystal structure, various novel heterostructures can be readily synthesized via incomplete cation exchange.

For example, partial Cd^{2+} exchange of spherical PbE (E = S, Se, Te) forms PbE/CdE core−shell nanocrystals displaying a type-I structure, improving their optoelectronic performance and environmental stability.[36] The mild conditions required for this surface cation exchange reaction enable the formation of PbE/CdE core/shell nanocrystals with negligible ripening of the seed particle, a common complication associated with traditional overcoating procedures of PbE. As the substitution of Pb^{2+} with Cd^{2+} is thermally activated, the thickness of the CdE shell can be controlled by varying the reaction temperature. The cubic phase of the parent PbE is bestowed upon the CdE shell with high fidelity during the exchange, resulting in a core−shell structure with a small lattice mismatch.

The anisotropic nature (see above) of many cation exchange reactions can be utilized to generate diverse nanoheterostructures when partial exchanges are applied to anisotropic nanoparticles. As described above, the partial Cu^{+} exchange of CdS nanorods leads to highly asymmetric binary Cu_2S−CdS heterostructures.[31] Performing the Cu^{+} exchange on self-assembled, aligned CdS nanorods can be used to further increase the asymmetry of this exchange, forming nanorods with a single interface Cu_2S−CdS primed for directional charge separation and extraction.[60] Likewise, binary nanorod superlattices can be formed by partial Ag^{+} exchange of CdS nanorods,[30] and these complex heterostructure morphologies can be further elaborated to generate divalent metal chalcogenide superlattices via two sequential ion substitutions.[27] Heterostructures analogous to seeded rods but composed of two different cations within a common anion sublattice can also be synthesized via partial exchange. Due to the preference of the Cd^{2+} exchange of lead chalcogenides to progress along the ⟨111⟩ direction, partial Cd^{2+} exchange of anisotropic PbS or PbSe rods forms PbE−CdE (E = S, Se) single and multiple dot-in-rod heterostructures,[37,61] which are practically impossible to access by conventional hot-injection synthesis methods.

The common requirement for heteroepitaxy during traditional seeded growth is relaxed considerably for cation exchange reactions. Indeed, single crystalline semiconductor shells can be formed around metal cores through nonepitaxial growth.[62] For example, the large lattice mismatch between CdS and Au (43%) would preclude the formation of conformal Au/CdS core/shell structures by traditional methods. However, the Cd^{2+}, Pb^{2+}, or Zn^{2+} cation exchange of amorphous, conformal Ag_2S shells surrounding Au cores generates the desired Au/CdS, Au/PbS, and Au/ZnS heterostructures, respectively, despite the fact that the metal chalcogenide shells are not in lattice registry with the gold core.

Synthesis of Doped Nanomaterials. The above examples illustrate the utility of quantitative and substoichiometric cation exchange. At severe substoichiometry, cation exchange can be used to incorporate low concentrations of defects or dopants into an otherwise pure nanocrystal host. The ability to controllably dope semiconductors with impurities allows the modulation of electronic,[63,64] optical,[65,66] and magnetic properties[67] of nanocrystals. However, development of hot-injection syntheses for the formation of impurity-doped nanocrystals has been challenging.[68] Kinetic competition between dopant inclusion and further overgrowth of the host material typically leads to much lower concentrations of dopants in the particle than in solution. Furthermore, the addition of dopants during the synthesis alters nucleation and growth kinetics, greatly complicating nanocrystal syntheses.[69,70] Postsynthetic control of doping via cation exchange is, therefore, highly desirable. As the size, shape, and quality of the nanocrystal host are retained during the exchange reaction, the influence of the impurity and its concentration on the nanocrystal's properties can be investigated in a controlled fashion. Fine-grained control over the number of impurities introduced by cation exchange can be achieved by regulating either the stoichiometry or kinetics of the ion substitution reaction.

Metal impurity doping of InAs nanocrystals was achieved by exposing InAs nanocrystals to dilute solutions of dissolved Ag, Cu, and Au salts.[41] The postsynthetic incorporation of these ions into the InAs host lattice likely occurs by substitution of In^{3+} with Au^{3+} or Ag^{+} or the formation of interstitial Cu^{+} ions. Using scanning tunneling spectroscopy (STS), the effects of the impurities on the electronic properties and Fermi level of the InAs nanocrystals were systematically probed (Figure 5). STS spectra reveal that the Fermi level and band structure remain largely unchanged upon isovalent Au^{3+} substitution. However, incorporation of interstitial Cu^{+} and substitutional Ag^{+} led to large changes in the Fermi energy and the formation of midgap

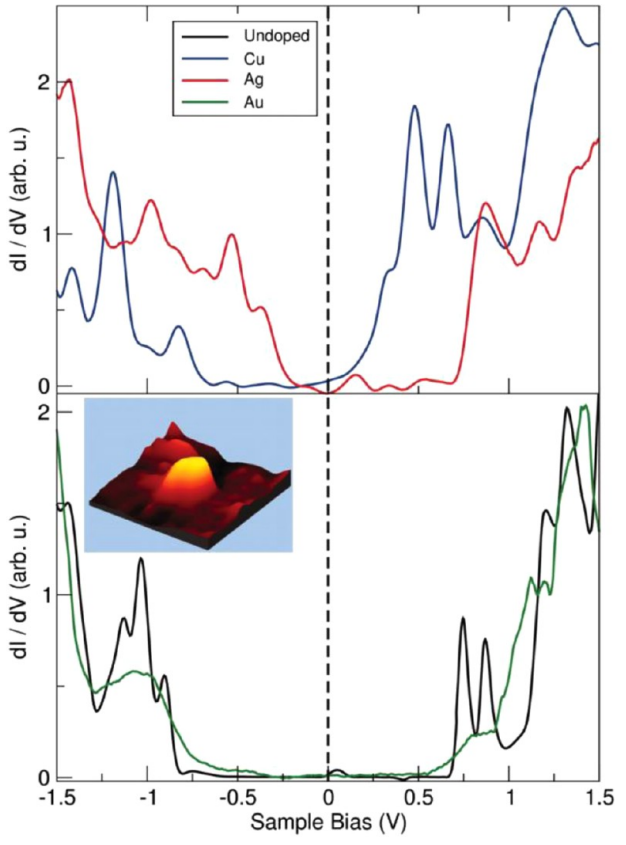

Figure 5. Scanning tunneling microscopy (STM) tunneling spectra of undoped (black trace), Au-doped (green trace), Cu-doped (blue trace), and Ag-doped (red trace) InAs nanocrystals, highlighting the relative shifts of the band edges in the doped samples. The inset shows an STM image of a single nanocrystal. Reproduced with permission from ref 41, copyright 2011 AAAS.

dx.doi.org/10.1021/jp405989z | J. Phys. Chem. C 2013, 117, 19759−19770

states. The creation of these midgap states and the associated shift in the Fermi energy suggests that ion exchange may be a promising strategy for the controlled doping of nanocrystals.

Cation exchange has also been utilized to dope CdSe with Ag^+.[71] Utilizing conditions similar to the reverse exchange reaction from $Ag_2Se \rightarrow CdSe$, CdSe nanocrystals were exposed to Ag^+ in the presence of a large excess of a trialkyl phosphine. Preferential phosphine ligation to Ag^+ reduced the driving force for ion substitution, permitting the controlled incorporation of Ag^+ impurities at concentrations as low as ~1 Ag^+ per nanocrystal. This methodology has been extended to Ag^+ doping of PbSe films, demonstrating its broad applicability to synthesizing electronically active materials.[72]

Cation exchange has also been employed to incorporate magnetically active dopants, such as Co^{2+} and Mn^{2+}. Co^{2+} doping in iron oxide nanocrystals is achieved by selective substitution of Fe^{2+} by Co^{2+}, permitting the modulation of the magnetic properties of the hematite host due to the stronger spin−orbit coupling of Co^{2+} sites.[73] The valence selectivity of this exchange reaction has been utilized to selectively dope the core of core/shell $FeO/CoFe_2O_4$ nanoparticles with Co^{2+} without modifying the Fe^{3+}-containing shell. Analogously, the commonly employed magnetically active dopant, Mn^{2+}, can also be incorporated by cation exchange.[74] ZnTe magic size nanocrystals exposed to a Mn(II) precursor at elevated temperature display characteristic emission of a Mn^{2+} dopant level in a ZnTe matrix, indicating successful ion substitution.

In Situ Cation Exchange Syntheses. While we have, thus far, drawn stark distinctions between conventional hot-injection synthesis and cation exchange, it is important to highlight the overlap between these two methods. Clearly, the template nature of cation exchange requires robust methods, such as hot-injection synthesis, for accessing high-quality nanocrystal scaffolds. However, in situ cation exchange, in which cation exchange reactions are combined in a one-pot fashion with conventional synthetic methods, may provide better synthetic control and enable the development of novel nanocrystals. One such strategy involves applying cation exchange to generate the desired seed particles in situ for immediate use in a subsequent growth step. In this approach, nucleation and growth can be temporally separated to achieve highly monodisperse nanocrystals. For example, a highly reactive precursor of one metal cation can efficiently nucleate nanocrystals of a different metal cation, provided rapid exchange occurs, as successfully demonstrated for the formation of monodisperse PbSe nanocrystals using the Sn(II) precursor, $Sn[N(SiMe_3)_2]$.[75] Additionally, multicomponent heterostructures can be synthesized by in situ cation exchange followed by seeded growth. The hot injection of large cubic phase $Cu_{2-x}Se$ nanocrystals into a reaction mixture optimized for CdS growth leads to the rapid exchange of $Cu_{2-x}Se \rightarrow CdSe$ with the growth of CdS shells nucleated by the newly formed CdSe seed particles.[76] The particular habit of the $Cu_{2-x}Se$ seed is transferred to the CdSe seed upon exchange, leading to the nucleation of octagonally symmetric CdS arms, resulting in unique CdSe/CdS octapods.

In situ cation exchange can further be utilized at intermediate stages of nanocrystal growth. The combination of conventional growth and conformal surface exchange can provide a method for radial engineering of nanocrystal composition using a simple one-pot method. For example, applying the surface-selective Hg^{2+} exchange of growing CdS nanocrystals leads to the formation of CdS/HgS/CdS quantum dots, colloidal nanocrystal analogues to thin-film quantum well structures.[77] These surface exchanges also provide a simple route for the creation of buffer layers to minimize lattice mismatch during overcoating procedures, preventing the formation of misfit dislocations that lead to deleterious effects on optical quality.[78] The in situ Ga^{3+} surface exchange on InP nanocrystals alters the lattice parameter sufficiently to permit epitaxial growth of ZnS shells, yielding highly luminescent nanocrystals.[79]

SUMMARY AND OUTLOOK

In summary, cation exchange reactions have proven to be an invaluable synthetic tool for accessing colloidal semiconductor nanocrystals of diverse composition, phase, and morphology. The ability to easily tune reaction thermodynamics via preferential ion ligation in solution has enabled nanocrystal cation exchange reactions with a great diversity of metal ions, including Ag^+,[7] Au^{3+},[41] Bi^{3+},[14] Cd^{2+},[7] Co^{2+},[73] Cu^+,[31] Cu^{2+},[7] Eu^{3+},[80] Ga^{3+},[48,79] Gd^{3+},[80] Hg^{2+},[49,77] In^{3+},[48] La^{3+},[80] Mn^{2+},[74] Pb^{2+},[25,27] Pt^{2+},[19] Pd^{2+},[19] Sb^{3+},[14] and Zn^{2+}.[25,26] Furthermore, the mild reaction conditions attendant to most exchanges make it a particularly powerful strategy for accessing many nonequilibrium morphologies, crystal phases, and materials that are difficult to prepare by direct hot-injection methods. Control over the extent of the exchange reaction further extends the utility of cation exchange for accessing a wide variety of heterostructures and doped nanocrystals.

The continued development of cation exchange as a synthetic tool would benefit from additional studies of the fundamentals of the exchange reaction. Accurate quantification of overall reaction thermodynamics and ligand binding energies is needed to enable the rational design of nanocrystal ion exchanges spanning the periodic table. In situ observation of reaction intermediates in nanocrystal ion exchanges would serve to clarify lingering mechanistic questions. These studies may benefit from recent advances in in situ TEM observation in the liquid phase.[81,82] Additional studies of nanocrystal ion exchange kinetics are essential to establish a unifying mechanistic picture across a broad range of anion host lattices, exchanging ions, and ligating environments. In this regard, the influence of surface ligation and its role in inhibiting or catalyzing ion exchange reactions remain underinvestigated. While cation exchange reactions have, thus far, largely focused on ionic metal chalcogenide phases, future work should expand the focus toward a broader class of nanomaterials inaccessible by direct synthetic methods.

AUTHOR INFORMATION

Corresponding Author

*E-mail: alivis@berkeley.edu.

Notes

The authors declare no competing financial interest.

Biographies

Brandon Beberwyck received his B.S. in Mechanical Engineering from the University of Texas at Austin in 2009 and his M.S. degree in Materials Science and Engineering at the University of California Berkeley in 2011. He is currently a Ph.D. student in the Alivisatos group, researching novel synthesis and fundamentals of ion exchange reactions in semiconductor nanocrystals.

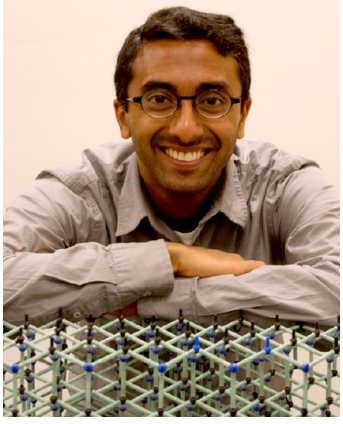

Yogesh (Yogi) Surendranath received a B.S. in Chemistry and B.A. in Physics from the University of Virginia in 2006, where he conducted research in the laboratory of W. Dean Harman. In 2011, he received a Ph.D. in Inorganic Chemistry from MIT in the laboratory of Daniel G. Nocera, where he studied electrocatalytic oxygen evolution mediated by metal oxide based thin-film catalysts. He is currently a Miller Postdoctoral Fellow in the Alivisatos group at the University of California Berkeley.

Paul Alivisatos is currently the Samsung Distinguished Professor of Nanoscience and Nanotechnology at the University of California Berkeley and serves as the seventh director of Lawrence Berkeley National Laboratory. He received a Bachelor's degree in Chemistry from the University of Chicago in 1981 and Ph.D. in Chemistry from UC Berkeley in 1986 prior to postdoctoral work with Louis Brus at AT&T Bell Laboratories. In 2004, he was elected into the National Academy of Sciences and the American Academy of Arts and Science. He is a fellow of the AAAS, ACS, APS, and MRS and the Co-Editor of Nano Letters. His research concerns the fundamental physical and chemical properties of nanocrystals and also works to develop practical applications of these new materials in biomedicine and renewable energy.

■ ACKNOWLEDGMENTS

This work and A.P.A. support provided by the Physical Chemistry of Inorganic Nanostructures Program, KC3103, Director, Office of Science, Office of Basic Energy Sciences, of the United States Department of Energy under contract DE-AC02-05CH11231. B.J.B. acknowledges support from the Department of Energy Office of Science Graduate Fellowship Program (DOE SCGF), made possible in part by the American Recovery and Reinvestment Act of 2009 and administered by ORISE-ORAU under DOE contract number DE-AC05-06OR23100. Y.S. acknowledges the Miller Institute for Basic Research in Science for a postdoctoral fellowship. We thank the many past and present group members whose research has contributed to the development of cation exchange in semiconductor nanocrystals.

■ REFERENCES

(1) Alivisatos, A. P. Perspectives on the Physical Chemistry of Semiconductor Nanocrystals. *J. Phys. Chem.* **1996**, *100*, 13226−13239.
(2) Yin, Y.; Alivisatos, A. P. Colloidal Nanocrystal Synthesis and the Organic−Inorganic Interface. *Nature* **2005**, *437*, 664−670.
(3) Park, J.; Joo, J.; Kwon, S. G.; Jang, Y.; Hyeon, T. Synthesis of Monodisperse Spherical Nanocrystals. *Angew. Chem., Int. Ed.* **2007**, *46*, 4630−4660.
(4) Talapin, D. V.; Lee, J.-S.; Kovalenko, M. V.; Shevchenko, E. V. Prospects of Colloidal Nanocrystals for Electronic and Optoelectronic Applications. *Chem. Rev.* **2010**, *110*, 389−458.
(5) Han, Z.; Qiu, F.; Eisenberg, R.; Holland, P. L.; Krauss, T. D. Robust Photogeneration of H_2 in Water Using Semiconductor Nanocrystals and a Nickel Catalyst. *Science* **2012**, *338*, 1321−1324.
(6) Michalet, X.; Pinaud, F. F.; Bentolila, L. A.; Tsay, J. M.; Doose, S.; Li, J. J.; Sundaresan, G.; Wu, A. M.; Gambhir, S. S.; Weiss, S. Quantum Dots for Live Cells, in Vivo Imaging, and Diagnostics. *Science* **2005**, *307*, 538−544.
(7) Son, D. H.; Hughes, S. M.; Yin, Y.; Alivisatos, A. P. Cation Exchange Reactions in Ionic Nanocrystals. *Science* **2004**, *306*, 1009−1012.
(8) Rivest, J. B.; Jain, P. K. Cation Exchange on the Nanoscale: An Emerging Technique for New Material Synthesis, Device Fabrication, and Chemical Sensing. *Chem. Soc. Rev.* **2013**, *42*, 89−96.
(9) Putnis, A. Mineral Replacement Reactions: From Macroscopic Observations to Microscopic Mechanisms. *Mineral. Mag.* **2002**, *66*, 689−708.
(10) Schmalzried, H. *Solid State Reactions*; Verlag Chemie: Weinheim, Germany, 1981.
(11) Fedorov, V. A.; Ganshin, V. A.; Korkishko, Y. N. Ion Exchange in II-VI Crystals: Thermodynamics, Kinetics, and Technology. *Phys. Status Solidi A* **1993**, *139*, 9−65.
(12) Osakada, K.; Yamamoto, T. Transmetallation of Alkynyl and Aryl Complexes of Group 10 Transition Metals. *Coord. Chem. Rev.* **2000**, *198*, 379−399.
(13) Dloczik, L.; Engelhardt, R.; Ernst, K.; Fiechter, S.; Sieber, I.; Könenkamp, R. Hexagonal Nanotubes of ZnS by Chemical Conversion of Monocrystalline ZnO Columns. *Appl. Phys. Lett.* **2001**, *78*, 3687−3689.

(14) Dloczik, L.; Könenkamp, R. Nanostructure Transfer in Semiconductors by Ion Exchange. *Nano Lett.* **2003**, *3*, 651−653.
(15) Park, J.; Zheng, H.; Jun, Y.-W.; Alivisatos, A. P. Hetero-Epitaxial Anion Exchange Yields Single-Crystalline Hollow Nanoparticles. *J. Am. Chem. Soc.* **2009**, *131*, 13943−13945.
(16) Yin, Y.; Rioux, R. M.; Erdonmez, C. K.; Hughes, S. M.; Somorjai, G. A.; Alivisatos, A. P. Formation of Hollow Nanocrystals Through the Nanoscale Kirkendall Effect. *Science* **2004**, *304*, 711−714.
(17) Dutt, M. B.; Sharma, B. L. *3 Diffusion in Compound Semiconductors*; Beke, D. L., Ed.;SpringerMaterials—The Landolt-Börnstein Database (http://www.springermaterials.com). DOI: 10.1007/10426818_10.
(18) Lokhande, C. D.; Gadave, K. M. A Simple Chemical Method for Conversion of CdS into Ag_2S and CdSe into Ag_2Se. *Mater. Chem. Phys.* **1993**, *36*, 119−123.
(19) Wark, S.; Hsia, C.-H.; Son, D. H. Effects of Ion Solvation and Volume Change of the Reaction on the Equilibrium and Morphology in Cation-Exchange Reaction of Nanocrystals. *J. Am. Chem. Soc.* **2008**, *130*, 9550−9555.
(20) Collaboration: Scientific Group Thermodata Europe (SGTE). *Thermodynamic Properties of Compounds*; SpringerMaterials - The Landolt-Börnstein Database (http://www.springermaterials.com).
(21) Vanysek, P. Electrochemical Series. In *CRC Handbook of Chemistry and Physics*, 87th ed.; Lide, D. R., Ed.; CRC Press: Boca Raton, FL, 2006; pp 8/20− 8/29.
(22) Engelken, R. D.; Ali, S.; Chang, L. N.; Brinkley, C.; Turner, K.; Hester, C. Study and Development of a Generic Electrochemical Ion-Exchange Process to Form M_xS Optoelectronic Materials from ZnS Precursor Films Formed by Chemical-Precipitation Solution Deposition. *Mater. Lett.* **1990**, *10*, 264−274.
(23) Chaudhry, M.; Persson, I. Transfer Thermodynamic Study on the Copper(II) Ion from Water to Methanol, Acetonitrile, Dimethyl Sulfoxide and Pyridine. *J. Chem. Soc., Faraday Trans.* **1994**, *90*, 2243−2248.
(24) Pearson, R. G. Absolute Electronegativity and Hardness: Application to Inorganic Chemistry. *Inorg. Chem.* **1988**, *27*, 734−740.
(25) Camargo, P. H. C.; Lee, Y. H.; Jeong, U.; Zou, Z.; Xia, Y. Cation Exchange: A Simple and Versatile Route to Inorganic Colloidal Spheres with the Same Size but Different Compositions and Properties. *Langmuir* **2007**, *23*, 2985−2992.
(26) Li, H.; Zanella, M.; Genovese, A.; Povia, M.; Falqui, A.; Giannini, C.; Manna, L. Sequential Cation Exchange in Nanocrystals: Preservation of Crystal Phase and Formation of Metastable Phases. *Nano Lett.* **2011**, *11*, 4964−4970.
(27) Luther, J. M.; Zheng, H.; Sadtler, B.; Alivisatos, A. P. Synthesis of PbS Nanorods and Other Ionic Nanocrystals of Complex Morphology by Sequential Cation Exchange Reactions. *J. Am. Chem. Soc.* **2009**, *131*, 16851−16857.
(28) Backhaus-Ricoult, M. Solid-State Reactivity at Heterophase Interfaces. *Annu. Rev. Mater. Res.* **2003**, *33*, 55−90.
(29) Jain, P. K.; Amirav, L.; Aloni, S.; Alivisatos, A. P. Nanoheterostructure Cation Exchange: Anionic Framework Conservation. *J. Am. Chem. Soc.* **2010**, *132*, 9997−9999.
(30) Robinson, R. D.; Sadtler, B.; Demchenko, D. O.; Erdonmez, C. K.; Wang, L.-W.; Alivisatos, A. P. Spontaneous Superlattice Formation in Nanorods Through Partial Caiton Exchange. *Science* **2007**, *317*, 355−358.
(31) Sadtler, B.; Demchenko, D. O.; Zheng, H.; Hughes, S. M.; Merkle, M. G.; Dahmen, U.; Wang, L.-W.; Alivisatos, A. P. Selective Facet Reactivity During Cation Exchange in Cadmium Sulfide Nanorods. *J. Am. Chem. Soc.* **2009**, *131*, 5285−5293.
(32) Demchenko, D. O.; Robinson, R. D.; Sadtler, B.; Erdonmez, C. K.; Alivisatos, A. P.; Wang, L.-W. Formation Mechanism and Properties of CdS-Ag_2S Nanorod Superlattices. *ACS Nano* **2008**, *2*, 627−636.
(33) Chan, E. M.; Marcus, M. A.; Fakra, S.; ElNaggar, M.; Mathies, R. A.; Alivisatos, A. P. Millisecond Kinetics of Nanocrystal Cation Exchange Using Microfluidic X-ray Absorption Spectroscopy. *J. Phys. Chem. A* **2007**, *111*, 12210−12215.
(34) Kubaschewski, O. Silver-Cadmium-Sulfur. In *Ternary Alloys: a Comprehensive Compendium of Evaluated Constitutional Data and Phase Diagrams*; Petzow, G., Effenberg, G., Eds.; VCH: Weinheim, 1988; Vol. *1*, pp 419−428.
(35) Mizetskaya, I. B.; Oleinik, G. S.; Trishchuk, L. I. Phase Diagram of the Cu_2S-CdS System. *Inorg. Mater.* **1982**, *18*, 581−582.
(36) Pietryga, J. M.; Werder, D. J.; Williams, D. J.; Casson, J. L.; Schaller, R. D.; Klimov, V. I.; Hollingsworth, J. A. Utilizing the Lability of Lead Selenide to Produce Heterostructured Nanocrystals with Bright, Stable Infrared Emission. *J. Am. Chem. Soc.* **2008**, *130*, 4879−4885.
(37) Casavola, M.; van Huis, M. A.; Bals, S.; Lambert, K.; Hens, Z.; Vanmaekelbergh, D. Anisotropic Cation Exchange in PbSe/CdSe Core/Shell Nanocrystals of Different Geometry. *Chem. Mater.* **2012**, *24*, 294−302.
(38) Bals, S.; Casavola, M.; van Huis, M. A.; Van Aert, S.; Batenburg, K. J.; Van Tendeloo, G.; Vanmaekelbergh, D. Three-Dimensional Atomic Imaging of Colloidal Core-Shell Nanocrystals. *Nano Lett.* **2011**, *11*, 3420−3424.
(39) Lambert, K.; De Geyter, B.; Moreels, I.; Hens, Z. PbTe|CdTe Core|Shell by Cation Exchange, a HR-TEM Study. *Chem. Mater.* **2009**, *21*, 778−780.
(40) Mokari, T.; Aharoni, A.; Popov, I.; Banin, U. Diffusion of Gold into InAs Nanocrystals. *Angew. Chem., Int. Ed.* **2006**, *45*, 8001−8005.
(41) Mocatta, D.; Cohen, G.; Schattner, J.; Millo, O.; Rabani, E.; Banin, U. Heavily Doped Semiconductor Nanocrystal Quantum Dots. *Science* **2011**, *332*, 77−81.
(42) Dorn, A.; Allen, P. M.; Harris, D. K.; Bawendi, M. G. In Situ Electrical Monitoring of Cation Exchange in Nanowires. *Nano Lett.* **2010**, *10*, 3948−3951.
(43) Peng, X.; Manna, L.; Yang, W.; Wickham, J.; Scher, E.; Kadavanich, A.; Alivisatos, A. P. Shape Control of CdSe Nanocrystals. *Nature* **2000**, *404*, 59−61.
(44) Manna, L.; Milliron, D. J.; Meisel, A.; Scher, E. C.; Alivisatos, A. P. Controlled Growth of Tetrapod-Branched Inorganic Nanocrystals. *Nat. Mater.* **2003**, *2*, 382−385.
(45) Puzder, A.; Williamson, A. J.; Zaitseva, N.; Galli, G.; Manna, L.; Alivisatos, A. P. The Effect of Organic Ligand Binding on the Growth of CdSe Nanoparticles Probed by Ab Initio Calculations. *Nano Lett.* **2004**, *4*, 2361−2365.
(46) Heath, J. R.; Shiang, J. J. Covalency in Semiconductor Quantum Dots. *Chem. Soc. Rev.* **1998**, *27*, 65−71.
(47) Allen, P. M.; Walker, B. J.; Bawendi, M. G. Mechanistic Insights into the Formation of InP Quantum Dots. *Angew. Chem., Int. Ed.* **2009**, *49*, 760−762.
(48) Beberwyck, B. J.; Alivisatos, A. P. Ion Exchange Synthesis of III-V Nanocrystals. *J. Am. Chem. Soc.* **2012**, *134*, 19977−19980.
(49) Smith, A. M.; Nie, S. Bright and Compact Alloyed Quantum Dots with Broadly Tunable Near-Infrared Absorption and Fluorescence Spectra Through Mercury Cation Exchange. *J. Am. Chem. Soc.* **2011**, *133*, 24−26.
(50) Zhong, X.; Feng, Y.; Zhang, Y.; Gu, Z.; Zou, L. A Facile Route to Violet- to Orange-Emitting $Cd_xZn_{1-x}Se$ Alloy Nanocrystals via Cation Exchange Reaction. *Nanotechnology* **2007**, *18*, 385606.
(51) De Trizio, L.; Prato, M.; Genovese, A.; Casu, A.; Povia, M.; Simonutti, R.; Alcocer, M. J. P.; D'Andrea, C.; Tassone, F.; Manna, L. Strongly Fluorescent Quaternary Cu−In−Zn−S Nanocrystals Prepared from $Cu_{1-x}InS_2$ Nanocrystals by Partial Cation Exchange. *Chem. Mater.* **2012**, *24*, 2400−2406.
(52) Carbone, L.; Cozzoli, P. D. Colloidal Heterostructured Nanocrystals: Synthesis and Growth Mechanisms. *Nano Today* **2010**, *5*, 449−493.
(53) Hines, M. A.; Guyot-Sionnest, P. Synthesis and Characterization of Strongly Luminescing ZnS-Capped CdSe Nanocrystals. *J. Phys. Chem.* **1996**, *100*, 468−471.
(54) Peng, X.; Schlamp, M. C.; Kadavanich, A. V.; Alivisatos, A. P. Epitaxial Growth of Highly Luminescent CdSe/CdS Core/Shell Nanocrystals with Photostability and Electronic Accessibility. *J. Am. Chem. Soc.* **1997**, *119*, 7019−7029.

(55) Kim, S.; Fisher, B.; Eisler, H.-J.; Bawendi, M. Type-II Quantum Dots: CdTe/CdSe(Core/Shell) and CdSe/ZnTe(Core/Shell) Heterostructures. *J. Am. Chem. Soc.* **2003**, *125*, 11466−11467.
(56) Talapin, D. V.; Nelson, J. H.; Shevchenko, E. V.; Aloni, S.; Sadtler, B.; Alivisatos, A. P. Seeded Growth of Highly Luminescent CdSe/CdS Nanoheterostructures with Rod and Tetrapod Morphologies. *Nano Lett.* **2007**, *7*, 2951−2959.
(57) Carbone, L.; Nobile, C.; De Giorgi, M.; Sala, F. D.; Morello, G.; Pompa, P.; Hytch, M.; Snoeck, E.; Fiore, A.; Franchini, I. R.; Nadasan, M.; Silvestre, A. F.; Chiodo, L.; Kudera, S.; Cingolani, R.; Krahne, R.; Manna, L. Synthesis and Micrometer-Scale Assembly of Colloidal CdSe/CdS Nanorods Prepared by a Seeded Growth Approach. *Nano Lett.* **2007**, *7*, 2942−2950.
(58) Li, H.; Brescia, R.; Krahne, R.; Bertoni, G.; Alcocer, M. J. P.; D'Andrea, C.; Scotognella, F.; Tassone, F.; Zanella, M.; De Giorgi, M.; Manna, L. Blue-UV-Emitting ZnSe(Dot)/ZnS(Rod) Core/Shell Nanocrystals Prepared from CdSe/CdS Nanocrystals by Sequential Cation Exchange. *ACS Nano* **2012**, *6*, 1637−1647.
(59) Jain, P. K.; Beberwyck, B. J.; Fong, L.-K.; Polking, M. J.; Alivisatos, A. P. Highly Luminescent Nanocrystals From Removal of Impurity Atoms Residual From Ion-Exchange Synthesis. *Angew. Chem., Int. Ed.* **2012**, *51*, 2387−2390.
(60) Rivest, J. B.; Swisher, S. L.; Fong, L.-K.; Zheng, H.; Alivisatos, A. P. Assembled Monolayer Nanorod Heterojunctions. *ACS Nano* **2011**, *5*, 3811−3816.
(61) Justo, Y.; Goris, B.; Kamal, J. S.; Geiregat, P.; Bals, S.; Hens, Z. Multiple Dot-in-Rod PbS/CdS Heterostructures with High Photoluminescence Quantum Yield in the Near-Infrared. *J. Am. Chem. Soc.* **2012**, *134*, 5484−5487.
(62) Zhang, J.; Tang, Y.; Lee, K.; Ouyang, M. Nonepitaxial Growth of Hybrid Core-Shell Nanostructures with Large Lattice Mismatches. *Science* **2010**, *327*, 1634−1638.
(63) Orlinskii, S.; Schmidt, J.; Baranov, P.; Hofmann, D.; de Mello Donegá, C.; Meijerink, A. Probing the Wave Function of Shallow Li and Na Donors in ZnO Nanoparticles. *Phys. Rev. Lett.* **2004**, *92*, 047603.
(64) Roy, S.; Tuinenga, C.; Fungura, F.; Dagtepe, P.; Chikan, V.; Jasinski, J. Progress Toward Producing n-Type CdSe Quantum Dots: Tin and Indium Doped CdSe Quantum Dots. *J. Phys. Chem. C* **2009**, *113*, 13008−13015.
(65) Bhargava, R. N.; Gallagher, D.; Hong, X.; Nurmikko, A. Optical Properties of Manganese-Doped Nanocrystals of ZnS. *Phys. Rev. Lett.* **1994**, *72*, 416−419.
(66) Pradhan, N.; Goorskey, D.; Thessing, J.; Peng, X. An Alternative of CdSe Nanocrystal Emitters: Pure and Tunable Impurity Emissions in ZnSe Nanocrystals. *J. Am. Chem. Soc.* **2005**, *127*, 17586−17587.
(67) Bryan, J. D.; Gamelin, D. R. Doped Semiconductor Nanocrystals: Synthesis, Characterization, Physical Properties, and Applications. *Prog. Inorg. Chem.* **2005**, *54*, 47−126.
(68) Norris, D. J.; Efros, A. L.; Erwin, S. C. Doped Nanocrystals. *Science* **2008**, *319*, 1776−1779.
(69) Tuinenga, C.; Jasinski, J.; Iwamoto, T.; Chikan, V. In Situ Observation of Heterogeneous Growth of CdSe Quantum Dots: Effect of Indium Doping on the Growth Kinetics. *ACS Nano* **2008**, *2*, 1411−1421.
(70) Beulac, R.; Ochsenbein, S. T.; Gamelin, D. R. Colloidal Transition-Metal-Doped Quantum Dots. In *Nanocrystal Quantum Dots*; Klimov, V. I., Ed.; CRC Press: Boca Raton, FL, 2010; pp 397−453.
(71) Sahu, A.; Kang, M. S.; Kompch, A.; Notthoff, C.; Wills, A. W.; Deng, D.; Winterer, M.; Frisbie, C. D.; Norris, D. J. Electronic Impurity Doping in CdSe Nanocrystals. *Nano Lett.* **2012**, *12*, 2587−2594.
(72) Kang, M. S.; Sahu, A.; Frisbie, C. D.; Norris, D. J. Influence of Silver Doping on Electron Transport in Thin Films of PbSe Nanocrystals. *Adv. Mater.* **2012**, *25*, 725−731.
(73) Sytnyk, M.; Kirchschlager, R.; Bodnarchuk, M. I.; Primetzhofer, D.; Kriegner, D.; Enser, H.; Stangl, J.; Bauer, P.; Voith, M.; Hassel, A. W.; Krumeich, F.; Ludwig, F.; Meingast, A.; Kothleitner, G.; Kovalenko, M. V.; Heiss, W. Tuning the Magnetic Properties of Metal Oxide Nanocrystal Heterostructures by Cation Exchange. *Nano Lett.* **2013**, *13*, 586−593.
(74) Eilers, J.; Groeneveld, E.; de Mello Donegá, C.; Meijerink, A. Optical Properties of Mn-Doped ZnTe Magic Size Nanocrystals. *J. Phys. Chem. Lett.* **2012**, *3*, 1663−1667.
(75) Kovalenko, M. V.; Talapin, D. V.; Loi, M. A.; Cordella, F.; Hesser, G.; Bodnarchuk, M. I.; Heiss, W. Quasi-Seeded Growth of Ligand-Tailored PbSe Nanocrystals Through Cation-Exchange-Mediated Nucleation. *Angew. Chem., Int. Ed.* **2008**, *47*, 3029−3033.
(76) Deka, S.; Miszta, K.; Dorfs, D.; Genovese, A.; Bertoni, G.; Manna, L. Octapod-Shaped Colloidal Nanocrystals of Cadmium Chalcogenides via "One-Pot" Cation Exchange and Seeded Growth. *Nano Lett.* **2010**, *10*, 3770−3776.
(77) Mews, A.; Eychmüller, A.; Giersig, M.; Schooss, D.; Weller, H. Preparation, Characterization, and Photophysics of the Quantum Dot Quantum Well System CdS/HgS/CdS. *J. Phys. Chem.* **1994**, *98*, 934−941.
(78) Dabbousi, B. O.; Rodriguez-Viejo, J.; Mikulec, F. V.; Heine, J. R.; Mattoussi, H.; Ober, R.; Jensen, K. F.; Bawendi, M. G. (CdSe)ZnS Core−Shell Quantum Dots: Synthesis and Characterization of a Size Series of Highly Luminescent Nanocrystallites. *J. Phys. Chem. B* **1997**, *101*, 9463−9475.
(79) Kim, S.; Kim, T.; Kang, M.; Kwak, S. K.; Yoo, T. W.; Park, L. S.; Yang, I.; Hwang, S.; Lee, J. E.; Kim, S. K.; Kim, S.-W. Highly Luminescent InP/GaP/ZnS Nanocrystals and Their Application to White Light-Emitting Diodes. *J. Am. Chem. Soc.* **2012**, *134*, 3804−3809.
(80) Dong, C.; van Veggel, F. C. J. M. Cation Exchange in Lanthanide Fluoride Nanoparticles. *ACS Nano* **2008**, *3*, 123−130.
(81) Zheng, H.; Smith, R. K.; Jun, Y.-W.; Kisielowski, C.; Dahmen, U.; Alivisatos, A. P. Observation of Single Colloidal Platinum Nanocrystal Growth Trajectories. *Science* **2009**, *324*, 1309−1312.
(82) Yuk, J. M.; Park, J.; Ercius, P.; Kim, K.; Hellebusch, D. J.; Crommie, M. F.; Lee, J. Y.; Zettl, A.; Alivisatos, A. P. High-Resolution EM of Colloidal Nanocrystal Growth Using Graphene Liquid Cells. *Science* **2012**, *336*, 61−64.